

THE INFLUENCE OF HYDROSTATIC PRESSURE ON FRACTURE

D. Francois*

ABSTRACT

Fracture in metals is commonly the result of plastic deformation, and as a whole, hydrostatic pressure does not influence macroscopic plastic flow. However, the microscopic processes of deformation and fracture are inhomogeneous and pressure can thus have an effect - the effect increasing with increasing inhomogeneity of the process. Thus, cleavage fracture is more influenced by pressure at the stage of grain boundary crossing than at the earlier stage of nucleation by Zener mechanism. Beryllium is an example of such a behaviour. Intergranular decohesion can be treated in the same manner. Ductile crack nucleation, the result of strain hardening of the matrix, requires a higher critical strain under pressure. As for void growth it seems necessary that the specimen necks for pressure to have an effect. Examples of such behaviour are given for 7075 aluminium alloy and for spheroidal graphite cast iron. Pressure increases the fracture toughness through its effect on the microscopic processes. Experiments on these materials are reported. The results are compared with various theoretical predictions, relating the fracture toughness to the microscopic processes at the crack tip.

INTRODUCTION

Until a rather recent time, there were few technological reasons to investigate the mechanical properties of materials under high pressure. As it was difficult to create such pressures, engineers worried about those conditions only when they occurred naturally and geologists were the first to deal with the problem of high pressures due to their existence within the earth's crust. However, with the progress of high pressure technology, it becomes advantageous to increase the working pressure of such apparatus as chemical synthesis reactors or nuclear reactors or to use pressure as a forming tool.

Notwithstanding these practical applications, our main interest in those studies stems from the fundamental understanding they can give us on the fracture phenomenon [1]. As it proceeds through the nucleation and growth of holes, which increase the volume of the fracturing material, hydrostatic pressure has a strong influence on fracture. It hinders the various microscopic fracture processes in different fashions and thus allows a better understanding of the critical steps. Linear elastic fracture mechanics does not predict any influence of pressure on fracture toughness. However it acts through its effect on the microscopic events which occur in the process zone. Thus hydrostatic pressure is a tool to check the models relating fracture toughness and microscopic fracture processes.

*Université de Technologie de Compiègne, Département de Génie Mécanique

As fracture is always the result of plastic deformation, some studies on this phenomenon under pressure will first be cited. Then work on the influence of pressure on microscopic processes such as cleavage or dimples formation and on fracture toughness will be reviewed. The experimental studies were carried out at Commissariat à l'Energie Atomique, Laboratoire de Bruyères le Chatel and they were conducted by a team including M. Contré, D. Carpentier, J.P. Auger, M. Gauthier and D. Rousseau of the Université de Technologie de Compiègne.

2. INFLUENCE OF PRESSURE ON ELASTIC DEFORMATION

It suffices to recall that as pressure brings the atoms closer together, it increases the influence of repulsive forces, and it leads to an increase of the elastic moduli. This variation does not exceed a few thousandths per 100 megapascal as checked many times [2, 3].

3. INFLUENCE OF PRESSURE ON PLASTIC DEFORMATION

3.1. Polycrystal. In the theory of plasticity the fundamental hypothesis that there is no volume change during plastic deformation is generally accepted. It is well justified by the negligible volume change which a dislocation introduces (about one atomic volume per interatomic distance along the line). For this reason, there is no work done against pressure when a dislocation is created, or when it moves, and pressure has a negligible effect on the flow stress [1]. This property has been checked on a number of metals such as beryllium [4], zinc, magnesium, cadmium, titanium, zirconium, cobalt [5] and uranium and some of its alloys [6] (Figure 1). As for these metals there is some anisotropy of the elastic constants, the plastic deformation is heterogeneous from grain to grain, at least at yield, and this might lead to detectable effects on the yield stress. But very precise measuring devices would be needed. At most it was noted that for beryllium, which exhibits two strain hardening stages, an increase of the transition strain with pressure is observed. This might be due to a higher resistance of the grain boundaries at high pressure produced by the accumulation of dislocations in their vicinity, or more simply to the occurrence of microcracks above a critical strain. Microcracking must be the explanation of the anomalous behaviour of spheroidal graphite cast iron (Figure 2). This material has a strain hardening coefficient which increases markedly under pressure. Our interpretation is that it is not connected with plastic deformation in itself but has to do with the opening up of holes at the interface between the graphite spheroids and the ferritic matrix.

3.2. Single crystals. It seemed appropriate to verify the results found on polycrystalline samples on single crystals. On beryllium it was observed [7] that pyramidal glide was not noticeably facilitated under pressure and that the critical shear stress on the basal plane was not changed, whereas it was slightly reduced on the prism plane. This was explained by an indirect effect of pressure which, increasing the line tension through its effect on the elastic constants, makes cross gliding easier. In spite of the fact that the number of active slip systems is not increased under pressure, as shown on Figure 1, the ductility becomes much larger: a polycrystal is thus able to deform a fair amount even though there are not 5 independent slip systems available.

4. MICROSCOPIC PROCESSES OF FRACTURE

4.1. General consideration. Cracks are created in a solid by stress concentrations which are the result of strain heterogeneity (glide bands, twins, second phase particles,...). The applied stress σ is locally multiplied by a stress concentration factor K_σ . The fracture stress is such that

$$K_\sigma \sigma_F^0 = \sigma^* \quad (1)$$

σ^* being the critical stress which must be reached locally. In a first approximation when a pressure p is superimposed the local stress becomes $(K_\sigma \sigma - p)$ and the fracture stress is now given by

$$(K_\sigma \sigma_F - p) = \sigma^* \quad (2)$$

which leads to

$$\sigma_F = \sigma_F^0 + p/K_\sigma \quad (3)$$

This relation shows that the influence of pressure is least for a strain heterogeneity which produces a large stress concentration. It is thus expected, for instance, that cleavage cracking which is produced by narrow glide bands or twins would be less affected than ductile fracture which results from a more diffuse strain leading to the opening of holes.

4.2. Cleavage fracture [8]. It is through the mechanism of Zener that the stress is concentrated at the head of dislocation pile ups and reaches the required high theoretical cleavage fracture stress ($\sim E/10$, E being Young's modulus). For metals this stress is an order of magnitude higher than the hydrostatic pressures usually available (~ 1000 MPa) so that there is a negligible effect on the nucleation of cleavage. However, this is not the case for cleavage crack propagation which is hindered. The effect is larger at the grain boundary crossing stage, when the cleavage crack is now long enough so that the strain heterogeneity is less apparent.

4.2.1. Cleavage crack nucleation. When a crack in a solid at pressure p is loaded by a superimposed uniaxial stress σ normal to the cleavage plane, the mean stress on the crack is

$$\sigma_\theta = \sigma - p + \sigma_D \quad (4)$$

where σ_D is the normal stress produced by the dislocations pile-up (or subgrain boundary, or twin). This stress σ_D is related to the effective shear stress on the glide plane $\tau_\alpha - \tau_i$

$$\sigma_D = D (\tau_\alpha - \tau_i) \quad (5)$$

where D is a function of the ratio L/a of the length of the pile up to the length of the crack, τ_α is the shear stress on the glide plane and τ_i is the friction stress on the dislocations. The cleavage crack nucleates when σ_θ reaches a critical value σ_c equal to the theoretical cleavage stress. Combining [4] and [5], the fracture stress σ_F is given by:

$$\sigma_F + D(\tau_\alpha - \tau_i) = \sigma_c + p \quad (6)$$

As σ_c is much larger than p in the usual laboratory experiments, the cleavage crack nucleation stress remains almost constant under pressure.

4.2.2. *Cleavage crack propagation.* Various models can be modified to introduce the influence of pressure. One example is the result obtained for the splitting of a tilt subgrain boundary [Friedel, Stroh, Gilman]. The stress needed for a cleavage crack to propagate within a grain is given by

$$(\tau_\alpha - \tau_i) (\sigma_\alpha - P) = \frac{4\gamma}{\pi B_{22} L} (\ln L/x + \delta) \quad (7)$$

In this formula $\tau_\alpha - \tau_i$ is the effective shear stress acting on the subgrain boundary dislocations, σ_α is the normal stress on the cleavage plane, γ is the fracture energy, L is the length of the subgrain boundary, x is the splitting distance and $\delta = 1 + \mu_2/\mu_1$ and B_{22} are functions of the elastic constants. The parenthesis in the right member of equation (7) has a value of approximately 4. The first grain where a cleavage crack propagates, is such that the normal to the cleavage plane makes an angle $\alpha = \alpha_F$ with the tensile axis. This critical value is close to $\pi/6$ at low pressure and it decreases as pressure is increased. The critical propagation stress σ_F is given by a parametric equation, α_F being the parameter. At high pressure it becomes proportional to the pressure p . Figure 3 shows an example of such a behaviour.

4.2.3. *Crossing the grain boundary.* When crossing the grain boundary the cleavage crack has the size of a grain, $2d$ and the stress needed at this stage can be calculated simply by using the Griffith formula;

$$\sigma_F - p = \left[\frac{\pi E \gamma_B}{(1-\nu^2)4d} \right]^{1/2} \quad (8)$$

where γ_B is the fracture energy for crossing the grain boundary. This energy is larger than γ for cleavage crack propagation. At high pressure it is this stage which becomes the harder and which controls fracture. The fracture stress is now proportional to the pressure. In beryllium, for some orientations, samples which were deformed under pressure indeed showed cracks which were stopped at grain boundaries [4].

4.3. *Intergranular decohesion.* Inasmuch as the intergranular decohesion is the result of stress concentrations at the head of dislocations pile ups on grain boundaries, it can be calculated using the model of Stroh [8]. The results must then be quite similar to those obtained for cleavage crack propagation. The cleavage fracture energy γ must be replaced by the grain boundary fracture energy γ_G . The interaction of dislocations pile ups in adjacent grains may have a stabilization effect which is favourable to the opening of grain boundary cracks. Thus can be explained the surprising occurrence of intergranular cracks parallel to the tensile axis in beryllium samples which were fractured under pressure [9]. In this case the extrusion texture plays an essential role. As it comes only from the effective shear stress on the basal glide planes this type of cracking is hardly modified under pressure. This observation might very well prove that cracking in beryllium is nucleated in grain boundaries and at atmospheric pressure immediately spread as cleavage cracks, masking the origin of brittleness.

4.4. Ductile fracture

4.4.1. *Void nucleation.* Argon, Im and Safoglu [10] studied the nucleation of voids at the interface between rigid inclusions and an elastoplastic matrix. They showed that the stress should reach a critical value σ_i at this interface through strain hardening in order to break the interface. Under a pressure p this value should be increased by this same amount p , so that a larger deformation is needed to reach it. If the stress-strain curve can be represented by the relation $\sigma = \sigma_0 \epsilon^n$ the elongation ϵ_F needed to break the interface is

$$\epsilon_F = \frac{(\sigma_i + p)^{1/n}}{\sigma_0} \quad (9)$$

and if σ_F/σ_F^0 is the ratio of the fracture stress under pressure to the fracture stress at atmospheric pressure

$$\sigma_F/\sigma_F^0 = 1 + p/\sigma_i \quad (9bis)$$

4.4.2. *Void growth.* McClintock calculated the fracture strain ϵ_F corresponding to the joining of cylindrical voids growing by plastic deformation. According to this theory as soon as a lateral pressure acts on the holes they stop growing, and on the contrary they close down. Fracture could then only happen once the specimen necks which induces a decrease of the hydrostatic pressure. The maximum radial stress in the axis of the specimen is $\sigma_y \ln(1 + a/2R)$, a being the minimum radius of the neck and R the radius of the generatrix and σ_y the elastic limit. If p is larger than this value, fracture is no longer possible. Using the empirical Bridgman linear relation between the ratio $a/2R$ and the maximum elongation at fracture ϵ_F , a relation can be deduced between ϵ_F and the ratio P/σ_y .

$$\left(\frac{1 + k \epsilon_F}{1 + k \epsilon_F^0} \right) = e^{p/\sigma_y} \quad (10)$$

with $k \epsilon_F = a/2R$.

McClintock also studied fracture by the growth of shear bands between the voids. The corresponding critical strain is obviously independent of pressure. It is an upper bound which would be proportional to the strain hardening coefficient. It is a current observation that under pressure the specimen necks down and that fracture occurs by macroscopic shearing of the reduced section.

4.4.3. *Ductile fracture of 7075 aluminium alloy.* The influence of pressure on the ductility of a 7075 T 651 aluminium alloy was studied both on cylindrical specimens 3 mm in diameter and with a 26 mm gauge length, and on 1 mm thick plane strain tensile specimens [11]. TR, TW, WR and RW orientations with respect to the rolling direction were tested. There was a difference between the uniaxial tensile ductility and the plain strain ductility which was partly reduced if the average tensile stress was subtracted out of the hydrostatic pressure. Indeed this average tensile stress is $\sigma/3$ in the uniaxial tensile test and $\sigma/2$ in the plane strain test. Still the plane strain ductility remained smaller than the uniaxial tensile ductility. According to Hahn and Rosenfield [12] the

ratio should be about 1/3 which was approximately true for all orientations except for the TR specimens where the ratio was closer to 1/2.

It can be argued that once the voids are nucleated the small additional deformation needed to break the specimen can be neglected. The measured value of the elongation at fracture ϵ_f could then be considered as the elongation needed to break the interface of the void nucleating inclusions. Figure 4 shows that relation (9bis) is well followed, giving a value of the breaking stress σ_i of 3000 MNm⁻² for TR and WR or RW specimens respectively. This difference must be related to the shape of the particles which are elongated in the rolling direction: it is easier to break the interface in the short transverse direction.

Relation (10) can also be checked by plotting ϵ_f/ϵ_f^0 against e^{p/σ_y} as in Figure 6. It again shows that the critical stress is greater for WR or RW specimens than for TR specimens.

4.4.4. *Ductile fracture of spheroidized graphite cast iron.* Experiments were conducted on spheroidized graphite cast iron with a ferritic matrix and 20 μ and 70 μ spheroids using plane strain tensile specimens.

Figure 5 shows the increase of the fracture stress as a function of pressure. Relation (9bis) is again well followed giving a value of the interface breaking stress of 1000 MPa. Figure 7 shows also that relation (10) is again obeyed.

5. INFLUENCE OF PRESSURE ON FRACTURE TOUGHNESS

5.1. *Macroscopic consideration.* The problem under study is concerned with the resistance to crack growth in cases where the pressurizing fluid can penetrate inside the crack. As the viscosity increases with pressure it is a question to know whether it can reach the crack tip. This can be checked by measuring the compliance which should vary as the inverse of the modulus of elasticity.

Applying a hydrostatic pressure alone to a cracked body does not produce any stress intensification at the crack tip. The stress intensity factor K does not change under pressure. G the crack extension force is multiplied by the ratio E_0/E of Young's modulus at atmospheric pressure to Young's modulus at pressure p , if Poisson's ratio ν is considered constant. The dimension R of the plastic zone at the crack tip being proportional to $(K/\sigma_y)^2$ does not vary under pressure, whereas the crack opening displacement, being proportional to G/σ_y , varies like E_0/E .

Thus the main influence of pressure on toughness comes from the change of the microscopic processes which operate in the process zone near the crack tip.

5.2. *Cleavage fracture.* Malkin and Tetelman [13] gave a relation between K_{IC} and the cleavage stress σ_f , the elastic limit σ_y and a structural parameter ρ_0 which has to do with the process zone size. It is deduced from the stress distribution in the plastic zone.

$$K_{IC} = 2.89 \sigma_y [\exp(\sigma_f/\sigma_y - 1) - 1]^{1/2} \sqrt{\rho_0} \quad (11)$$

Under pressure p this relation becomes

$$K_{IC} = 2.89 \sigma_y [\exp(\sigma_f + p)/\sigma_y - 1]^{1/2} \sqrt{\rho_0} \quad (12)$$

σ_f itself being a function of p (cf paragraph 4.2.). There is however one difficulty: the calculation of σ_f must take into account the influence of the average stress ahead of the crack tip at the place where the cleavage cracks start. At atmospheric pressure it varies between a tensile value of 1500 to 1850 MPa in the experiments reported by Malkin and Tetelman. For comparison purposes σ_f should be measured in like conditions, at the root of a notch for instance. Although to our knowledge there are no experiments relating K_{IC} to pressure, when cleavage is controlling, it can be predicted that K_{IC} will increase with pressure and that the transition temperature will be lowered.

5.3. Ductile fracture

5.3.1. *7075 aluminium alloy.* Figure 8 shows the influence of pressure on K_{IC} for TR specimens of 7075 aluminium alloy [11]. The experiments were conducted on 3 points bend and CT specimens. The ASTM validity conditions were not fulfilled above $K_{IC} = 26 \text{ MNm}^{-3/2}$. Nevertheless there is no doubt that K_{IC} increased with pressure as the specimens displayed wider and wider shear lips as pressure was increased. Figure 9 shows a plot of $\ln K_{IC}$ as a function of $\ln \epsilon_f$. K_{IC} is approximately proportional to $\epsilon_f^{1/2}$ (ϵ_f being measured in plane strain specimens). This is in keeping with a proposal of Barsom and Pellegrino [14] and of Hahn and Rosenfield [12]. These authors related the strain at the crack tip to the dimension of the plastic zone size and deduced

$$K_{IC} = (0.05 E \sigma_y n^2 \epsilon_f)^{1/2} \quad (13)$$

in S_I units n being the strain hardening coefficient.

In Figure 8 the solid line is given by this theory and in view of the approximations, the fit looks quite satisfactory.

However Rice and Johnson [15] proposed that the critical crack opening displacement δ_c should be equal to the average distance between the void nucleating inclusions. Using micrographs taken on various directions with respect to the rolling direction we evaluated the mean distance \bar{d} between inclusions along the most probable crack path. We calculated δ_c using the formulae

$$\delta_c = K_{IC}^2 / 2 E \sigma_y \quad (14)$$

At atmospheric pressure the plot of δ_c versus \bar{d} as shown in Figure 10 yields $\delta_c = 0.6\bar{d}$. The agreement with the theory is quite good. From the measured values of K_{IC} under pressure δ_c can then be calculated and using the above relation with \bar{d} , the mean distance between void nucleating inclusions can be found as a function of pressure. This distance increases, reaching for instance, 0.6 mm for RW specimens and 0.25 mm for TW specimens at 400 MPa. According to Argon et al. [10], the critical stress to break the interface is not a function of the radius of the particles, unless their distribution is heterogeneous. This is indeed what is observed in our specimens. The most closely spaced large particles are then the ones which create the first voids, because of the interaction between their plastic zones. The smaller particles act only at a later stage in the deformation. This would

then explain why under pressure those smaller particles would not nucleate voids, leading to a higher \bar{d} .

5.3.2. *Spheroidized graphite cast iron.* For this materials a phenomenon of stable crack growth complicated the measurement of K_{IC} . However, using the potential drop technique K_{Ii} at initiation of cracking could be determined at various pressures. The results are given in Table 1.

It turns out that there was some dispersion in the results but that there was no noticeable change of K_{Ii} under pressure. At least in that case the proportionality with $\epsilon_f^{1/2}$ was not observed and the theory of Hahn and Rosenfield was not the one to take into account. Now the critical COD at initiation was much smaller than the average distance between the graphite spheroids. Looking at Figure 11 which is a micrograph taken at the crack tip at the initiation stage, we propose that the crack initiation is related to the necking of the ligament between two closely spaced spheroids and a relation of the type

$$\delta_c \sim \Phi \cdot n \quad (15)$$

is expected Φ being the diameter of the spheroids and n the strain hardening coefficient of the ferritic matrix. It gives indeed the right order of magnitude for δ_c , and it explains why pressure has no effect at least until the breaking of the particle matrix interface is not too much increased.

CONCLUSION

We have confirmed that hydrostatic pressure in most cases affects only the ductility of metals, and the more so, the less heterogeneous is the deformation process which nucleates the cracks. It is the retardation of these processes which increases the fracture toughness under pressure. The study of these variations gives some clue as to the way the fracture toughness is related to the microscopic processes. The increases of fracture toughness with pressure is rather reassuring in the building of pressure vessels. On the other hand, there are some parts in structures where the average stress can be highly tensile. A back extrapolation might then show that the fracture toughness could decrease below the usual plane strain value [16].

REFERENCES

1. POIRIER, J.P., FRANCOIS, D. and ADDA, Y., Ann. Physc., 5, 1970, 291.
2. BARSCH, G.R., Phys. Stat. Soli., 19, 129, and BARSCH, G.R. and CHANG, Z.P., Phys. Stat. Soli., 19, 1967, 139.
3. CLANET, D., Commissariat à l'Energie Atomique, rapport D0.0012.U DT/MN.MP71 II.
4. BEDERE, D., JAMARD, C., JARLAUD, A. and FRANCOIS, D., Acta. Met., 19, 1971, 973.
5. CARPENTIER, D., Mechanical Tests Under Hydrostatic Pressures up to 15 kb, 25th Annual Meeting National Conference on Fluid Power, Chicago, 1969.
6. AUGER, J.P., rapport C.E.A., D0.0006-73-06.
7. BEDERE, D., JAMARD, C., JARLAUD, A., and FRANCOIS, D., Phys. Stat. Soli., (a) I, 1970, 135.
8. FRANCOIS, D. and WILSHAW, T.R., J. Appl. Phys., 39, 1968, 4170.
9. FRANCOIS, D., C.R. Acad. Sciences, Paris, 268, 1969, 580.
10. ARGON, A.S., IM, J. and SAFOGLU, R., Met. Trans., 6A, 1975, 825.
11. AUGER, J.P. and FRANCOIS, D., Revue de Phys. Appliquée, 9, 1974, 637.
12. HAHN, G.T. and ROSENFIELD, A.R., ASTM STP, 432, 1975, 5.
13. MALKIN, J. and TETELMAN, A.S., in "La Rupture des Métaux", Masson & Cie, Paris, 1972, 209.
14. BARSOM, J.M. and PELLEGRINO, J.V., Engng. Fract. Mech. 5, 1973, 209.
15. RICE, J.R. and JOHNSON, M.A., Elastic Behavior of Solids, McGraw Hill, New York, 1970.
16. AURICH, D., Engng. Fract. Mech., 7, 1975, 761.

Table 1

P MPa	a mm	K_{Ii} MPa \sqrt{m}	δ meas. μ	δ calc. μ
0.1	7.50	26.4	4	6
0.1	9.69	16.4	3	2.5
250	8.87	27.3	8	6
500	7.42	26.5	13.5	6
500	7.59	22.1	3	4
500	9.65	16.2	3.5	2
500	7.41	21.1	9	4
750	7.47	25.4	7.5	5.5
750	7.81	23.0	8	4.5

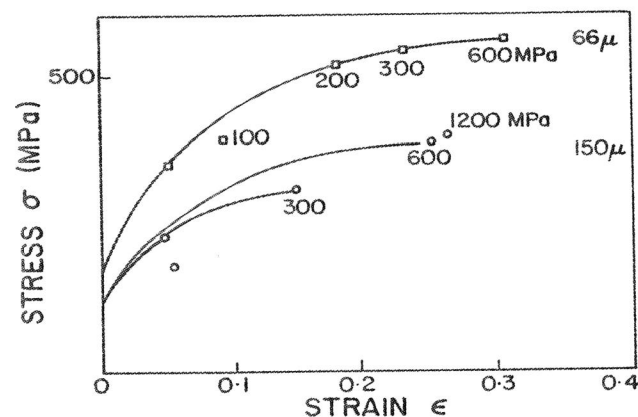


Figure 1 Influence of pressure on the stress strain curve of beryllium. With two different grain sizes [4].

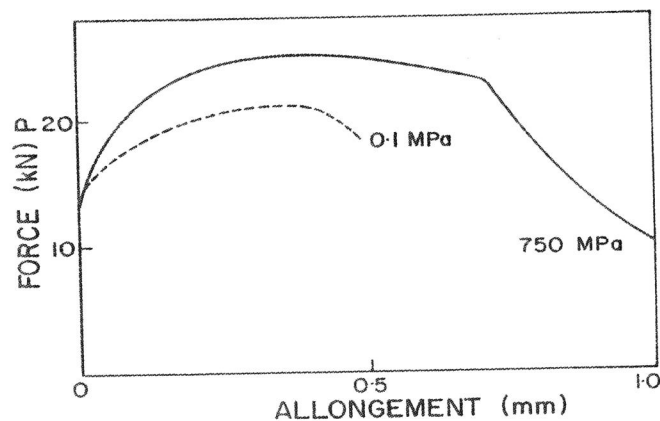


Figure 2 Anomalous behavior of spheroidized graphite cast iron under pressure. The strain hardening coefficient is increased.

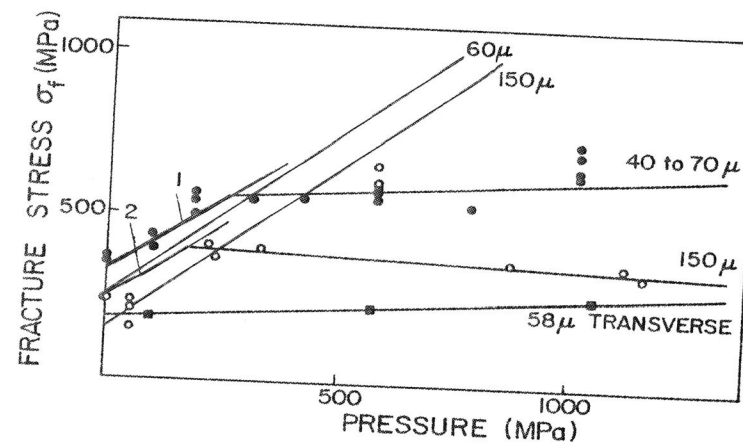


Figure 3 Evolution of the cleavage fracture stress as a function of pressure for beryllium [4].

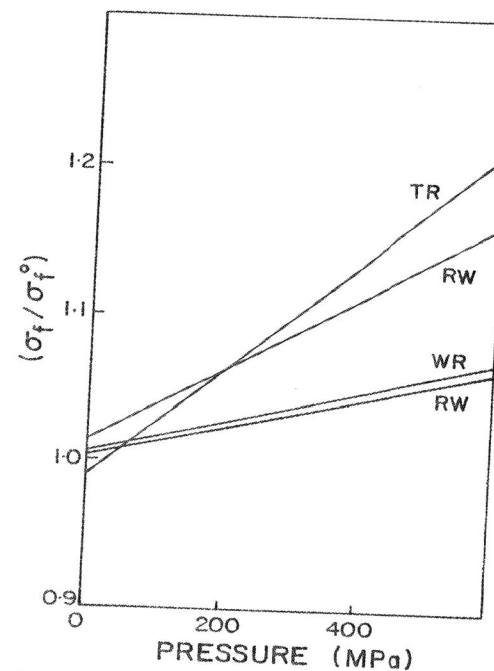


Figure 4 Plot of the ratio of the fracture stress under pressure to fracture stress at atmospheric pressure versus pressure for specimens of 7075 having various orientations with respect to the rolling direction.

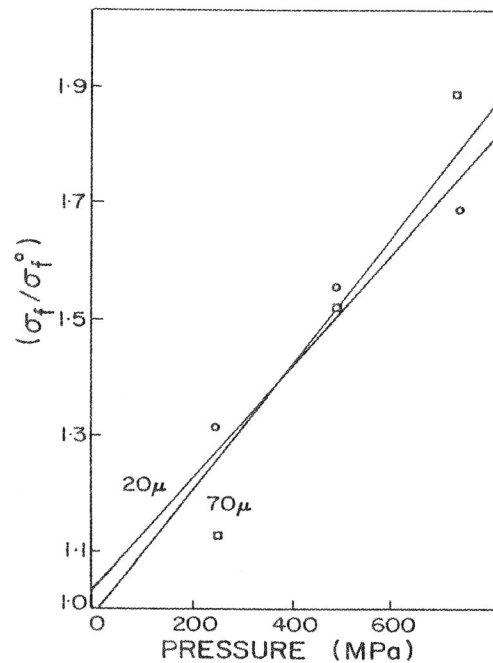


Figure 5 Plot of the ratio of the fracture stress under pressure to the fracture stress at atmospheric pressure versus pressure for specimens of spheroidized cast iron.

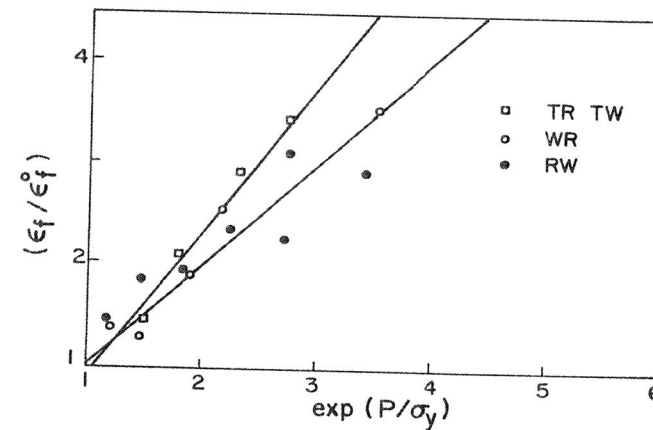


Figure 6 Plot of the ratio of the fracture strain under pressure to the fracture strain at atmospheric pressure versus $\exp P/\sigma_y$ for specimens of 7075 having various orientations with respect to the rolling direction.

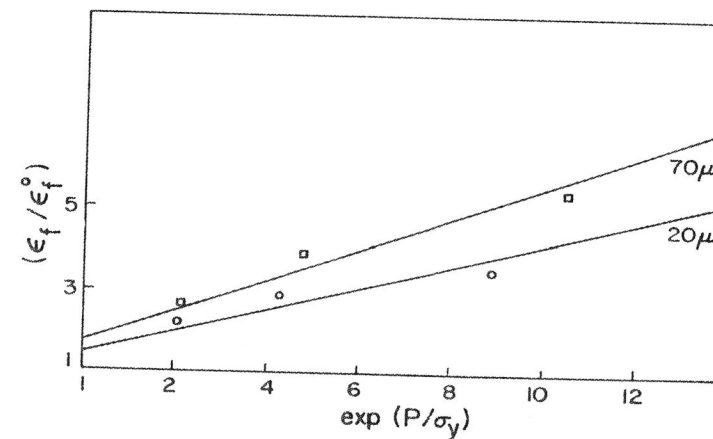


Figure 7 Plot of the ratio of the fracture strain under pressure to the fracture strain at atmospheric pressure versus $\exp P/\sigma_y$ for specimens of spheroidized cast iron.

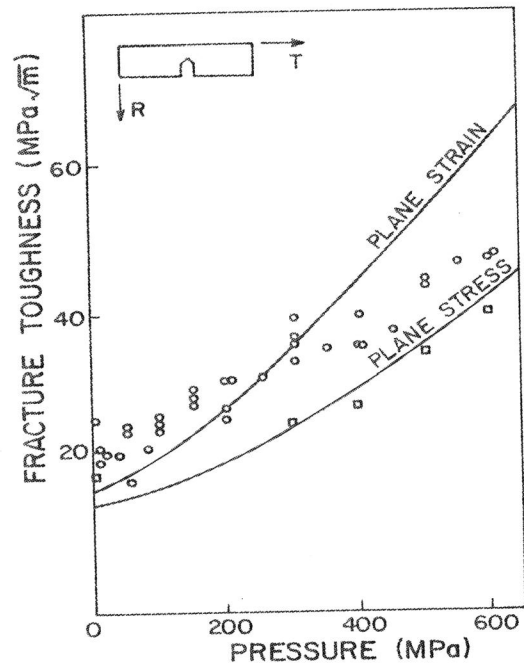


Figure 8 Evolution of K_{IC} for 7075 as a function of pressure for TR specimens. The solid line represents Hahn and Rosenfield's relation.

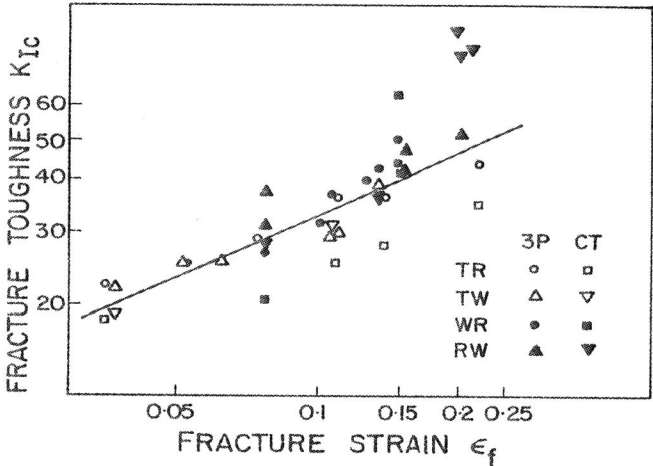


Figure 9 Log-log plot of K_{IC} versus the fracture strain ϵ_f

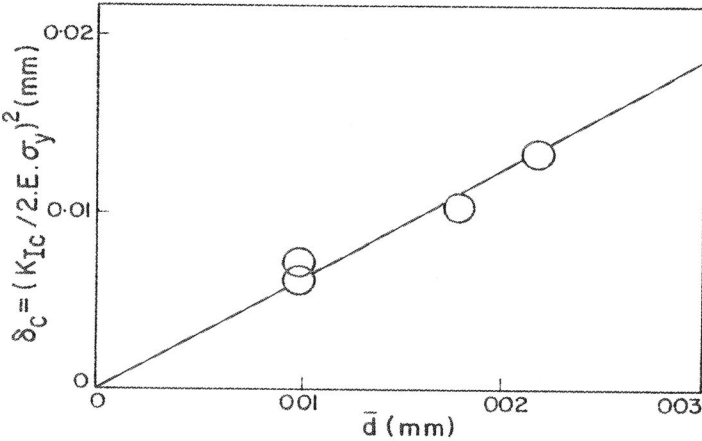


Figure 10 Plot of δ_c the crack opening displacement versus the average distance d between void nucleating inclusions.



Figure 11 Micrograph of a crack in spheroidized graphite cast iron showing necking between the closest spheroids